Journal of Materials Chemistry C

Accepted Manuscript

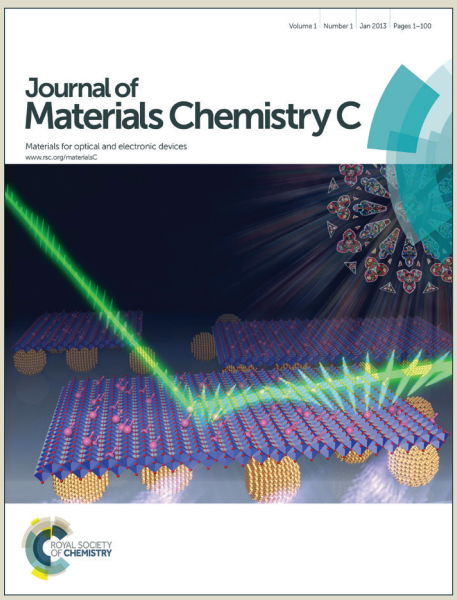

ROYAL SOCIETY OF CHEMISTRY

www.rsc.org/materialsC

Atomic Layer Deposition of Cu with a Carbene-Stabilized Cu (I) Silylamide

Authors: Dirk J. Hagen[1], Ian M. Povey[1], Simon Rushworth[1], Jacqueline S. Wrench[1], Lynette Keeney[1], Michael Schmidt[1], Nikolay Petkov[1], Sean T. Barry[2], Jason P. Coyle[2], and Martyn E. Pemble[1,3*]

Affiliations: [1]Tyndall National Institute, University College Cork, 'Lee Maltings', Dyke Parade, Ireland.

[2]Department of Chemistry, Carleton University, 1125 Colonel By Drive, K1S 5B6, Ottawa, Canada.

[3]Department of Chemistry, University College Cork, Cork, Ireland

[*]**Corresponding author:** martyn.pemble@tyndall.ie

Abstract: The metal-organic Cu(I) complex 1,3-diisopropyl-imidazolin-2-ylidene copper hexamethyl disilazide has been tested as a novel oxygen-free precursor for atomic layer deposition of Cu with molecular hydrogen. Being a strong Lewis base, the carbene stabilizes the metal centre to form a monomeric compound that can be vaporised and transported without visible degradation. A significant substrate dependence of the growth process not only with respect to the film material but also to the structure of the films was observed. On Pd surfaces continuous films are grown and no phase boundary can be observed between the Cu film and the Pd, while island growth is observed on Ru substrates, which as a consequence requires thicker films in order to achieve a fully coalesced layer. Island growth is also observed for ultra-thin (<10 nm) Pd layers on Si substrates. Possible explanations for the different growth modes observed are discussed.

1. Introduction

Apart from certain specific applications related to so-called front-end-of-line transistor fabrication [1–4] and the passivation of photovoltaic devices [5,6] atomic layer deposition (ALD) has been mainly developed as a useful tool for the study of a wide range of materials on the nanoscale [7–16], partly because the growth rates achievable are slow as compared to other growth techniques such as CVD [17–20] and PVD [21,22] methods. Perhaps, the most successful example is the oxide of the gate stack in a transistor architecture [1–4] where the performance of the device is very sensitive to the individual layer thickness [23]. Furthermore, as tri-gate and high-k on III-V techniques are introduced for transistors [24], ALD is especially beneficial due to its self-limiting nature and surface-cleaning effects [25–28].

For metals, successful ALD processing has been somewhat more limited. The platinum group metals Pt [29], Ir [30], Ru [31], Rh [32] and Os [33] can be deposited by an oxygen combustion ALD process, where the metal film catalyzes the oxidation of the ligands while the film remains metallic due to the lack of stability of their oxides. Tungsten has also been grown by ALD using a fluorosilane elimination reaction, which is well established for chemical vapour deposition (CVD) processes in the fabrication of microelectronic devices [34].

Among the remaining metals, Cu is arguably the one in which most research effort has been dedicated thus far. This is mainly due to the use of Cu for CMOS interconnects where the half-pitch of the first metallisation layer (metal-1) is predicted to be less than 10 nm within one decade [35]. Although there exist some reports using CuCl as a precursor for Cu ALD [36–38] most work has been carried out using metal-organic precursor molecules since the vapour pressure of Cu halides is very low. Within the metal-organic family, Cu (II)-diketonates have been the most intensively studied group. Cu (II) acetylacetonate ($Cu(acac)_2$) is a readily available molecule and has been

mainly used for plasma assisted ALD processes [39,40]. Thermal ALD has also been reported [41], but required temperatures as high as 250 °C. Although the derivative Cu (II) tetramethylheptanedionate ($Cu(tmhd)_2$) has the advantage of a slightly higher vapour pressure, results from ALD experiments are similar to those found with $Cu(acac)_2$, thermal ALD processing being limited to a small range of substrate materials (Pd, Pt) [42,43] or the use of plasma being necessary [44].

The fluorinated compound Cu (II) hexafluoroacetylacetonate ($Cu(hfac)_2$) has a reasonably higher vapour pressure but its most stable form is a monohydrate; accordingly it has found limited use in Cu ALD processing [45]. Furthermore, fluorine containing molecules are not favoured by the electronics industry as they can cause severe contamination. Recently, low temperature deposition has been reported with Cu (II)-bis-ketoiminates) [46–48] and Cu(II)-aminoalkoxides [46,49,50] but the reactions required the use of plasma [46,48] or of a relatively complicated reduction chemistry such as a transmetalisation [49] or the use of three-reagent cycles [50].

Cu (I)-metalorganics often react more readily to metallic Cu than Cu (II) compounds. For example Cu (I)-diketonates have long been studied as precursors for CVD with the hfac compound being the most commonly used diketo-ligand [51,52]. The main reaction mechanism is disproportionation:

$$2LCu(diket.) \rightarrow 2Cu(diket.)^* + 2L\uparrow \qquad (1)$$

$$2Cu(diket.)^* \rightarrow Cu^* + Cu(diket)_2\uparrow \qquad (2)$$

Here, L represents a dative ligand and asterisks describe surface species. Typical dative ligands include trimethylvinylsilyl (TMVS) [51], 1,5-cyclooctadiene (COD) [52,53] and 3,3-dimethyl-1-butene (DMB) [54,55]. It is clear that no ALD process can be realized with the reactions described by equations 1 and 2 as no surface saturation can be achieved. The situation is further complicated

by the observation that the complexes start to disproportionate under typical evaporation conditions. Norman et al. [56] mitigated this effect by adding an excess of TMVS as additives to the TMVS-Cu(hfac) precursor, but evaporation of the resulting solution required a more complex experimental arrangement such as direct liquid injection. Nevertheless, at the time of writing, Air Products are selling TMVS-Cu(hfac) as a solution containing additives under the trade name CupraSelect. The lack of saturated growth was also observed for other classes Cu (I) metalorganics such as diketiminates [57,58].

In this present work 1,3-diisopropyl-imidazolin-2-ylidene-Cu-bis(trimethylsilylamide) (NHC-Cu(hmds), figure 1) was evaluated for ALD. The hmds ligand contains neither oxygen nor halogens which are regarded as potentially problematic contaminants. Importantly, reaction of the precursor alone – specifically in the absence of any other oxygen-containing species- may not directly result in oxide formation. Furthermore, the possible by-product $Cu(hmds)_2$ is unlikely to be stable as linear configurations are very rare for Cu (II) complexes [59]. Therefore, a reaction similar to that described by equation 2 is not expected to take place. However, the tetramer $[Cu(hmds)]_4$ has been reported to be a stable compound [60] and although the CVD growth of Cu with $[Cu(hmds)]_4$ has been reported [60] its vapour pressure is low- possibly too low for any viable transport to occur under normal ALD or CVD conditions. Formation of the tetramer can be inhibited by the presence of the N-heterocyclic carbene 1,3-diisopropyl-imidazzolin-2-ylidene which is a strong σ donor as was demonstrated by Coyle et al. [61]. In this work this stabilised hmds precursor is evaluated for thermal ALD with molecular H_2 on various substrates. The reaction is proposed to proceed as follows:

$$\text{NHC-Cu(hmds)} \rightarrow \text{Cu(hmds)*} + \text{NHC}\uparrow \qquad (3)$$

$$1/2\text{H}_2 \rightarrow \text{H*} \qquad (4)$$

$$\text{Cu(hmds)*} + \text{H*} \rightarrow \text{Cu*} + \text{Hhmds}\uparrow \qquad (5)$$

The dissociative adsorption of H_2 on the substrate material and the reaction of the H* surface species with the adsorbed precursor are very surface selective. For example Martenstein and Carlsson [43] reported growth of Cu on an Pd/Pt alloy film but not on oxidized substrates when they used $Cu(tmhd)_2$ and molecular H_2. Jezewski et al. [44] needed a plasma source to achieve growth on Au on which H_2 does not dissociate.

2. Experimental

The precursor NHC-Cu(hmds) was synthesized according to the method described previously [61]. The compound has a melting point of 51 °C and a vapour pressure of 1 Torr at 131 °C.

ALD experiments were carried out in a home-built hot wall reactor. The reactor consisted of a 5 cm thick stainless steel tube which was positioned in a tube furnace. An inner glass tube was placed inside the steel tube in order to provide a relatively inert surface. Samples were placed on a stainless steel sample holder positioned in the middle of the tube. The precursor was heated in a 200 ml bubbler at 90 °C, yielding a vapour pressure of ca. 140 mTorr. N_2 was used as carrier gas as well as for purging the reactor. Three ALD valves (Swagelok) were used to direct the N_2 flow through the bubbler or bypassing it directly into the reactor. The pipes were heated to 140 °C to avoid condensation. The reactant was hydrogen diluted in argon (10 %). The flow of both, N_2 and H_2/Ar was controlled by mass flow controllers. The ALD valves were controlled by a computer program written with LabView.

For the Pd substrates, 15 nm Ti and 70 nm Pd were deposited by electron beam evaporation on Si wafers possessing 500 nm of thermal oxide. The film thickness was monitored with a quartz crystal microbalance (QMC). Titanium was employed as an adhesion layer, which was needed because Pd

would otherwise agglomerate at the relatively moderate temperatures used. For the thin Pd layers 5 nm Ti and <10 nm Pd were deposited with the same method. The Ru films were deposited by cold-sputtering on oxidized Si.

Scanning electron microscopy (SEM) micrographs were taken with a Quanta FEG 650 microscope in secondary electron mode. To determine the film thickness, cross-sectional micrographs were taken from an angle of 60°. Several measurements were taken with the image processing program ImageJ in order to determine a mean value. Energy dispersive x-ray spectroscopy (EDX) was carried out on the SEM using an Oxford Instruments X-Max detector using a acceleration voltage of 20 V.

X-ray diffraction (XRD) was carried out with Panalytical X'Pert PRO Materials Research Diffractometer in Bragg-Brentano geometry using Cu K alpha radiation with an x-ray mirror and the X'Celerator real time multiple strip (RTMS) detector.

Micro-structural analysis was performed using HR-TEM (Jeol 2100 transmission electron microscope; 200 kV; double tilt holder). Cross-sections of the films were prepared for micro-structural analysis using a FEI Dual-Beam Helios NanoLab 600i Focused Ion Beam (FIB) (final thinning at 93 pA 30 kV, final polish 2 kV 28 pA).

A commercial atomic force microscope (AFM)(MFP-3D, Asylum Research) in AC mode was used for topography mapping and roughness measurements of the films. Olympus AC160TS silicon cantilevers (Al reflex coated, ~300 kHz resonant frequency) were used for imaging.

3. Results and Discussion

3.1 Growth on Ruthenium

Ruthenium is a substrate material of considerable interest for back-end-of-line processing as it is a candidate to replace Ta as a liner material for Cu interconnects [62] on CMOS devices. Hydrogen adsorbs dissociatively on Ru, which is widely used as a catalyst for hydrogenation reactions [63]. Therefore, one might expect a Ru substrate to enable the reaction of the adsorbed precursor with molecular hydrogen over a wide temperature range. Figure 2 compares Cu films grown at 320, 240, 220, and 170 °C using 1000 cycles, except for the first sample where only 813 cycles were used. This relatively high temperature deposition experiment was performed during the initial testing of the precursor delivery system and although the variation in the number of cycles employed is not optimal the micrograph for the 813 cycle deposit is still is included here as it is a good example of Cu growth at high temperatures. At a substrate temperature of 320 °C the micrograph is dominated by large islands with smaller islands in between. The large, distant islands result from the longer migration path of surface species at high temperatures. This leaves much bare substrate space for new islands to nucleate and thus a large size distribution is observed. Furthermore, secondary grain growth mechanisms such as island migration, coalescence [64,65] and Ostwald-ripening [66,67] might play a role at such temperatures. With decreasing temperature nucleation gets denser and the grain size is more evenly distributed. At 170 °C the growth rate decreases suggesting that the reactivity of molecular hydrogen decreases significantly at this temperature and/or that the rate of precursor chemisorption also decreases. Chemisorption of the Cu precursor is likely to involve breaking of the Cu-Carbene bond which was calculated by Coyle et al. to require a dissociation energy of 293 kJ/mol [61]. Thus, activation of reaction 3 above is a reasonable possibility that has to be considered.

The densest deposit was obtained at 220 °C where the vertical diameter of the islands was measured from cross-sectional SEM micrographs to be about 40 nm. Taking into account the surface coverage, it is not unreasonable to estimate an effective film thickness that is somewhere between 1/3 and 2/3 of this value. This would correspond to a growth rate of between 0.13 and 0.27 Å/cycle.

In a previous unpublished study, we performed similar experiments with the conventional precursor $Cu(tmhd)_2$. As can be seen in figure 3 a much denser film is grown with the NHC-Cu(hmds) precursor at 220 °C. The nucleation density is expected to be dependent on temperature, adsorption density (number of partially reacted precursor molecules per unit area of substrate) and surface properties. One might expect a higher adsorption density for NHC-Cu(hmds) than for the more bulky $Cu(tmhd)_2$ compound due to steric effects. However, the precursor can also influence the nucleation density via other, chemical effects. For example the precursor can alter the properties of the substrate surface. As $Cu(tmhd)_2$ contains oxygen and has a tendency to coordinate to water it might oxidise the Ru surface to a certain degree. It is known that the degree of surface oxide formation of a metal substrate has a huge impact on the quality of the Cu film deposited on it [40]. For example, Moffat et al. [68] observed distinctive island growth during the direct electrochemical deposition of Cu on Ru when a surface oxide was present while continuous films was obtained after reducing the oxide.

The results were reproducible during a lengthy series of experiments indicating that the carbene group indeed prevented the formation of the tetramer and no significant decomposition took place in the bubbler over several weeks at elevated temperatures. Stability is a significant issue for Cu(I) compounds as discussed earlier. Waechtler et al. [69,70] used bis(tri-n-butylphosphine) to stabilize Cu (I) (acac) and reported its use for the ALD of copper oxide. Triethylphosphine has been used to stabilize Cu (I)-cyclopentadiene and the resulting compound was used for CVD experiments by

Senocq et al. [71]. However, although both groups reported no measurable P content, contamination is still a main issue when using phosphines as P increases the resistivity of Cu significantly. With this in mind we suggest that the carbene - stabilised precursor employed here represents a significant advancement in Cu (I) precursor chemistry since it demonstrates stabilisation without the need to use potentially problematic P-containing ligands.

Furthermore, it is noteworthy that we also carried out ALD experiments with Cu(hmds) that was not stabilised by any dative ligand. Although initial results from the first looked promising, the extent of growth diminished rapidly with continued use of the un-stabilised precursor. We postulate that this was due to remnants of monomeric Cu(hmds), which might have been partially stabilised by remnants of the solvent (ether), being present in the as-received compound, but this remains to be confirmed or denied.

3.2 Growth on Palladium

Growth characteristics such as change of thickness with the number of cycles (growth per cycle, GPC) or the dependence of the growth rate on temperature are important measures which are often used to describe an ALD process. Unfortunately, as shown in the previous section it was not possible to properly evaluate these parameters for the growth of Cu on Ru substrates using the NHC-Cu(hmds) precursor this as continuous thin films could not be grown. For this reason Pd was used as an alternative substrate in order to investigate further the role of metallic surfaces in the reaction in question. Pd is one of the few substrates for which thermal Cu ALD has been reported [42,43]. Pd is also employed as catalyst for hydrogenation [72,73] and so the same considerations may apply as described for the Ru surface in terms of the surface reacting with H_2 to produce atomic hydrogen. In addition Pd presents an oxide-free surface [43] which we believe may be a significant factor in the overall optimisation of the Cu ALD process.

Typical SEM micrographs of Cu films deposited on Pd are depicted in figure 4. In contrast to the results for Cu films on Ru, the deposited Cu could not be distinguished from the underlying Pd either in top view or in cross-section. Scanning of the composition of the films with EDX showed clearly the presence of Cu at reasonable levels and comparable Cu signals were detected all over the surface; thus, there is no evidence, at least from EDX, for the presence of any 'bare' Pd surface between the Cu grains at all temperatures studied (140 - 320 °C), although the spatial resolution of EDX is somewhat limited by the spot size of the electron beam of ca. 17 nm.

In order to examine the morphology of the films XRD was carried out in Bragg-Brentano geometry (figure 6). A clear Cu (111) peak could be seen at an approximate 2-theta value of 43° indicating that metallic Cu was deposited. The XRD patterns showed no evidence for a Cu (200) peak (at an approximate 2theta value of 50°) despite the fact that this peak is commonly observed to be the second largest peak for randomly oriented Cu [74]. This therefore suggests that the deposit was not randomly oriented and has a preferential (111) orientation. Similarly oriented growth was reported by Li and Gordon [75,76] for Cu ALD on Co. Hsu et al. reported a phase composition for their Cu films on Pd [42] but used in-plane grazing incidence XRD which does not provide information on the orientation perpendicular to the surface. Martensson and Carlsson [43] also reported diffraction data for their Cu films grown on a Pt/Pd alloy obtained using a grazing incident geometry where significant Cu (111) and Cu (200) signals indicated the presence of a disordered grain structure. Furthermore Hsu et al. also noted a shift of the Cu (111) peak towards lower angles with increasing temperature [42]. They interpreted this shift as being indicative of the formation of a CuPd phase (CuPd (220) peak) however such a shift could also be expected from the application of Vegard's law to the formation of a true solid solution of Cu and Pd [77].

As a discrete Cu film could not be distinguished from the underlying Pd in the SEM cross-section

micrographs the thickness of the combined film was measured. The growth rate was then determined by subtracting the thickness of the Ti/Pd seed layer (85 nm) and dividing by the number of cycles. The thickness of the substrate film was monitored during their deposition with a QCM and the thickness was confirmed by electron microscopy. The variation of growth rate with respect to temperature is shown in figure 6. Arguably, the growth rate is relatively stable between 190 and 250 °C at about 0.45 Å/cycle. Such a temperature window of constant growth rate is often used as a proof for an ALD process, although it is no requirement as for some ALD processes the saturated growth rate varies with temperature [30]. To investigate if film growth was indeed the result of surface saturation within this window, the length of the NHC-Cu(hmds) pulse was varied at 220 °C. The growth rate levels at about 0.45 Å/cycle, as can be seen in figure 7. This is a clear indication of saturated growth.

The growth rate increases significantly above 250 °C most likely as a result of the emergence of a CVD component resulting from pyrolysis of the precursor. Below 190 °C the growth rate decreases. Again this might be due to the low reactivity of molecular hydrogen and/or the lack of precursor adsorption. The latter can either be caused by the activation energy needed for chemisorption or by problems with the precursor transport due to condensation of the precursor on the reactor walls arising as a result of the significant temperature difference between the centre of the tube furnace and its ends. However, we believe the most likely reason for the decrease in growth is associated with the activation energy needed for at least one of the reactions in equations 3 - 5 since the temperature of the precursor inlet should not be low enough for significant condensation to occur under the conditions employed. Moreover, a decrease of the growth rate in this temperature range has been described for other Cu ALD processes employing H_2 [43].

Another important question to consider here is how the reaction proceeds after the Pd is covered with a Cu film. Although H_2 also adsorbs dissociatively on Cu [78,79] a significant activation

energy is associated with such a process. Kiyomiya et al. e.g. reported an activation energy of 38 kJ/mol for H_2 adsorption on Cu powder [78] and Tabatabaei et al. [79] 42 kJ/mol for adsorption on Cu on an alumina support. It is therefore possible to conclude, that given a reasonable value of the Arrhenius frequency factor, that the reaction might be expected to proceed efficiently at temperatures around 200 °C.

The relatively large deviation of measured thickness and growth rate is to a large part due to the roughness of the films, especially of those grown at high temperatures. An increase of roughness with temperature was confirmed with AFM measurements (micrographs not shown here). While the bare Pd film has a rms roughness of 0.91 nm, films grown at 160 °C with 950 cycles, 180 °C with 855 cycles, 220 °C with 800 cycles and 250 °C with 868 cycles the rms roughnesses were 2.1 nm, 3.0 nm, 4.5 nm and 7.6 nm, respectively. Annealing of a Pd sample at 220 °C for several hours by way of a control experiment resulted in no increase in surface roughness.

The relatively high thickness of the Pd layer and the associated roughness can also cause a significant error in the determination of the growth rate; consequently thinner films (~7 nm Pd on 5 nm Ti) were also used as substrates. To our surprise the formation of Cu islands similar in appearance to this formed on the Ru films was observed rather than the growth of continuous films as seen on the thicker (70 nm) Pd films as can be seen in figure 8.

At present the precise reason(s) for these observations are not known. However we may speculate that they may arise as a consequence of intermetallic solubility considerations and subsequent different phase bimetallic material formation. It is well known that Cu and Pd are very soluble in each other and that interdiffusion has been reported for Cu ALD on Pd [42]. This means that Cu atoms can join Pd grains instead of diffusing on the surface until nucleating with each other. On the other hand, Ru and Cu are completely insoluble in each other; thus, Cu atoms must diffuse across a

rigid surface and meet each other at more diverse nucleation points. However the very different behaviour observed between thick and thin Pd substrates is more surprising. The effect could arise due to the presence of different grain structures between the two films which in turn could dramatically influence the activation energy for diffusion of the two metals into each other. Supersaturation of Cu in the thin Pd films seems unlikely as the two metals form a complete solid solution with two intermetallic phases. We suggest here that these details are of fundamental interest in terms of the ALD of Cu on metallic surfaces although we also note that the solubility of Cu on Pd effectively render Pd ineffective in terms of it acting as a diffusion barrier.

Cross-sectional TEM was been carried out in order to investigate the differences between the interfaces of the films and structures deposited. In figure 9, micrographs taken at different resolution are presented for Cu deposited on the thick Pd substrates. The high resolution micrograph was taken from the Pd/Cu interface. While a sharp interface is clearly discernible between the Ti adhesion layer and the Pd layer the contrasts are much weaker between Cu and Pd. It is therefore very difficult to assess the nature of the interface as its appearance changes from visible to completely absent across the cross-section. However, the micrograph in figure 9c gives an indication for a gradual transition. The metallic nature of the deposited film was confirmed by selected area electron diffraction (SAED) as can be seen in figure 10.

TEM micrographs of Cu deposits grown at 220 °C on the Ru and ultra-thin Pd films are shown in figure 11. The islands obtained on Ru were crystalline and had a wetting angle of ca. 60°. The islands on Pd were also crystalline but had a much larger wetting angle of about 130°. The equilibrium wetting angle θ is described by Young's formula, equation 6:

$$\cos(\theta) = \frac{\gamma_{su} - \gamma_{if}}{\gamma_{Cu}} \qquad (6)$$

where γ_{su} is the surface energy of the substrate, γ_{if} the interface energy and γ_{Cu} the surface energy of the Cu deposit. From equation 6 one can see that the wetting angle decreases with increasing γ_{su} and decreasing γ_{if}. The former is phenomenological described as scaling with the melting point [80] while the latter increases with the mismatch of the interplanar spacing of the two materials δ [80]:

$$\delta = \frac{d_{Cu} - d_{su}}{d_{su}} \qquad (7)$$

where d_{Cu} and d_{su} are the interplanar spacing of the Cu film and the substrate, respectively. Kim et al. [80] investigated the wetting of Cu on Ru when deposited by PVD and observed an equilibrium angle of 43°. The angles observed in our experiments are slightly larger, being ca. 60°. Possible reasons for this apparent disparity with the data of Kim et al. include lack of understanding and control of the surface chemistry pertaining under ALD conditions as compared with PVD conditions together with possible differences of the crystal structure of the Ru films. While Kim et al. [80] used strongly (001) textured Ru films nano-crystalline films were used in this study. Smoother films were reported when Cu was grown by low temperature PEALD on (001) textured Ru than on nano-crystalline Ru [46].

A larger wetting angle for Cu grown on Pd as compared to that for Cu grown on Ru can be expected from equations 6 and 7 as the surface energy is lower and the interface energy with Cu higher due to the larger lattice mismatch (0.07 Cu(111)/Pd(111), 0.04 Cu(111)/Ru(002)).

In figure 11b a second, smaller island can be seen on the left side of the image. This island has a smaller wetting angle than that observed for the larger island. Furthermore, there is deposited material between the islands. Figure 11c shows this thin deposit which has a small wetting angle. These observations indicate the action of possible de-wetting effects during the film growth due to misfit strain relief, similar to that observed for Stranski-Krastanov type growth [81,82]. The large

islands have pronounced facets and are hexagonally shaped as can be seen in the TEM cross-section in figure 11b and the SEM plan-view in figure 8b. The expression for the island shape given in equation 6 is in a strict sense only valid for the wetting of liquids but can be applied to describe solid islands adequately in many cases. However, the anisotropy of the surface energy can have a strong impact on crystalline islands and result in the formation of facets. Hexagonal shapes were reported for nano-particles of metals with a cubic lattice such as Cu [83] and can be understood by the low surface energy of the (111) plane and the faster crystal growth in the (100) than in the (111) direction [84].

From this discussion the deposition of continuous Cu films that appear to wet the substrate effectively on thick Pd substrate films seems surprising. A possible explanation for this observation would be to invoke relaxation effects for example via the formation of a mixed interlayer as reported by Hsu et al. [42]. With this in mind we attempted to test for possible intermixing by carrying out transmission-EDX scans on cross-sectional samples. However, these experiments proved to be somewhat inconclusive as signals from scattering of emitted x-rays in the films seemed to be dominant. However, indications for a graded interlayer were found in high the resolution TEM investigations as discussed earlier. Furthermore, the shift of the Cu peak with temperature in the XRD measurements shown in figure 5 are also an indication of a graded interface since interdiffusion is a thermally activated process.

4. Conclusions

NHC-Cu(hmds) has been tested as a precursor for thermal Cu ALD with H_2. The reaction is assumed to involve chemisorption of the precursor by breaking of the Cu-NHC bond, dissociative adsorption of H_2 and reaction of the surface species to form Hhmds and metallic Cu.

On Ru substrates efficient growth was obtained above 200 °C. Upon increasing the temperature to 320 °C the island density decreased and the island size increased as expected for island growth. Below 200 °C growth was much less pronounced. Possible reasons for this include insufficient reactivity of molecular H_2 and/or a lack of breaking of the NHC-Cu bond. Future plasma-based ALD studies will enable us to probe these possibilities further. However, the results obtained demonstrated a clear improvement in growth morphology and control as compared to that obtained with conventional Cu (II)-metalorganics. When compared with other Cu (I) compounds NHC-Cu(hmds) showed good stability due to the strong Cu-NHC bond avoiding unwanted side reactions such as the formation of $[Cu(hmds)]_4$ during the evaporation process.

When growth was carried out on Pd substrates continuous films could be obtained. An ALD growth window was observed between 190 and 250 °C and some evidence was found for saturated growth with a GPC of ca. 0.4 Å/cycle at 220 °C by varying the precursor pulse time.

When ultra-thin Pd films were used islands were grown instead of continuous films. The islands had a larger wetting angle than those grown on Ru and had a less regular size distribution. A classical model which predicts that [80] larger wetting angles can be expected on Pd where no surface relaxation takes place is described. However, the existence of such a ‘rigid’ surface is questionable for the growth of Cu on Pd as both metals are miscible. The formation of a graded interface by inter-diffusion is a possible mechanism for the reduction of interface stresses and it can be argued that stress reduction can occur more readily in a relatively thick substrate film. Although we were not able to find direct evidence of a graded interlayer by EDX strong indications of the formation of such a layer were found from TEM analysis. Such a graded layer resulting from inter-diffusion between Cu and Pd during Cu ALD would be consistent with previous studies made under comparable conditions [42].

Acknowledgements

The support of Science Foundation Ireland via grant number 07/SRC/I112, FORME- Functional Oxides and Related Materials for Electronics, is gratefully acknowledged. We also gratefully acknowledge support for a studentship (DJH) from the Irish Research Council for Science, Engineering and Technology (IRCSET) and Intel Ireland. Finally we thank GreenCentre, Kingston, Canada, for supplying the Cu precursor.

Figures

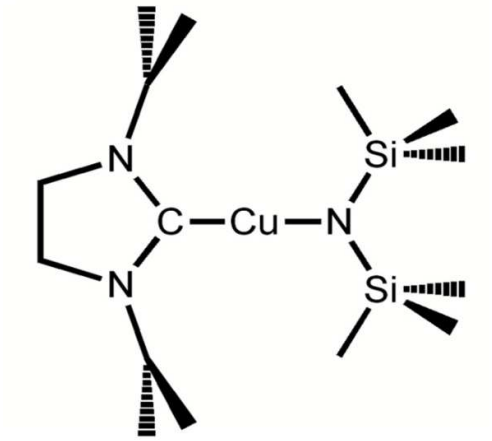

Figure 1: 1,3-diisopropyl-imidazolin-2-ylidene copper(I) hexamethyldisilazide

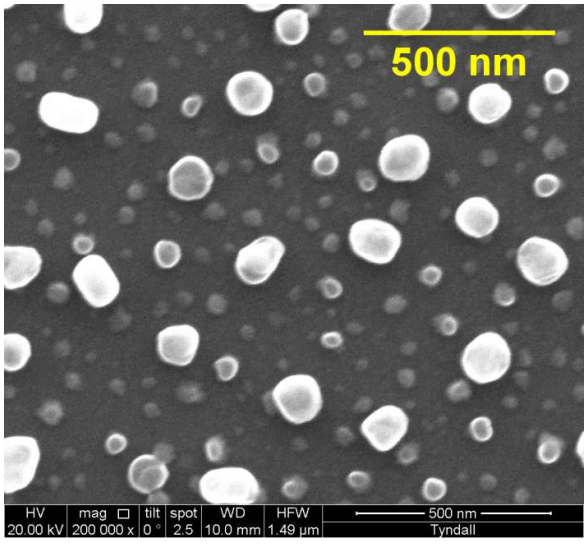

Figure 2 (a)

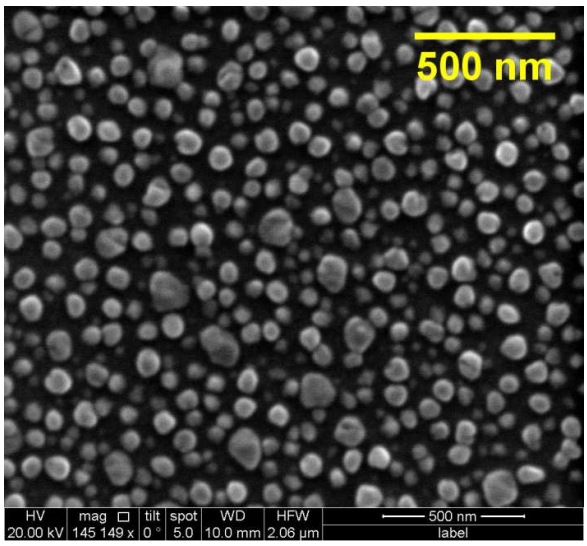

Figure 2 (b)

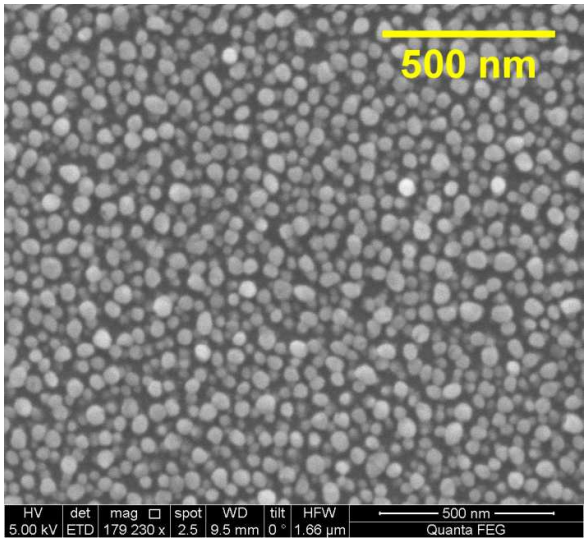

Figure 2 (c)

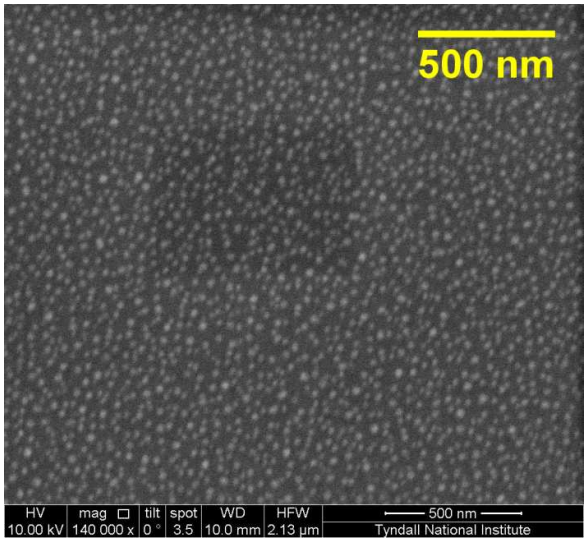

Figure 2 (d)

Figure 2: SEM micrographs of Cu deposits on Ru grown at (a) 320, (b) 240, (c) 220, and (d) 170 °C.

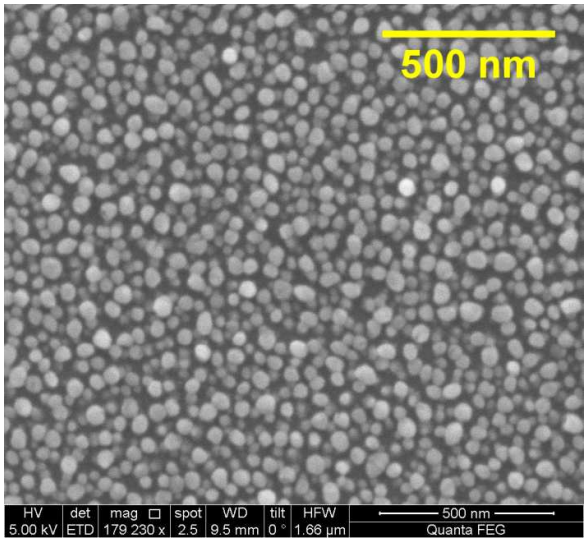

Figure 3 (a)

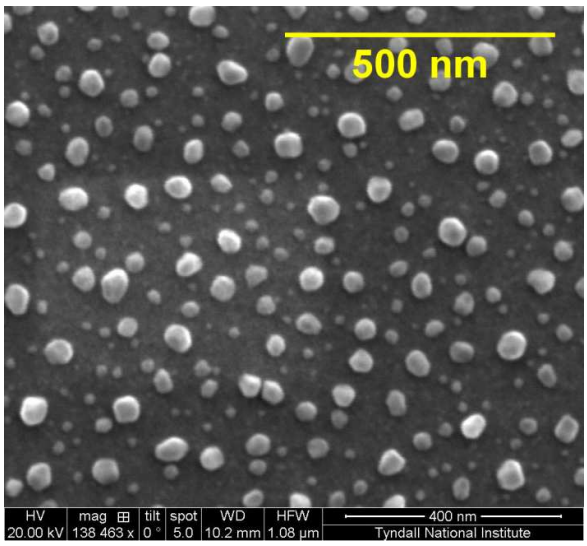

Figure 3 (b)

Figure 3: Comparison of results for Cu films deposited at 220 °C using (a) [NHC]Cu(hmds) and (b) $Cu(tmhd)_2$.

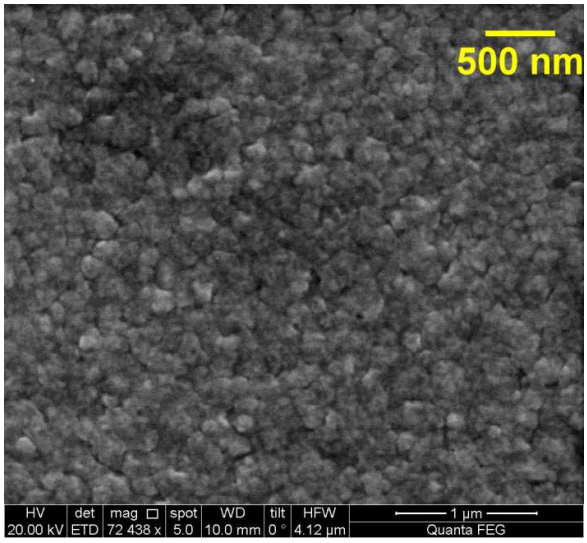

Figure 4 (a)

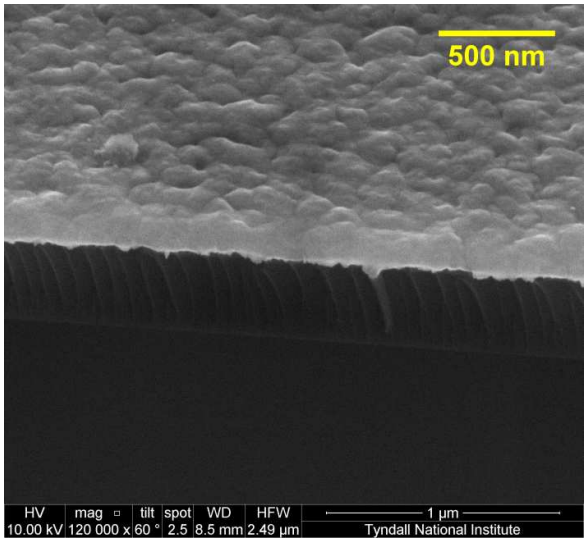

Figure 4 (b)

Figure 4 : SEM micrographs of Cu on Pd grown with 1000 cycles at 220 °C; (a) top-view, (b) cross-section.

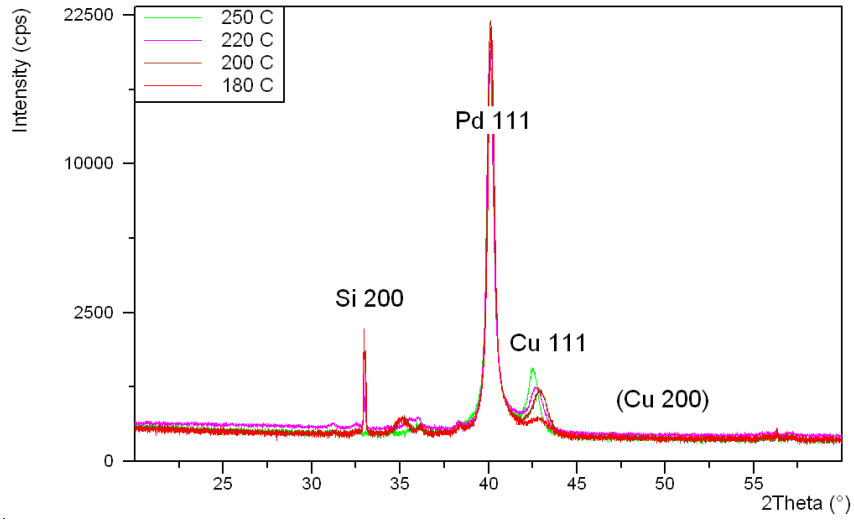

Figure 5 : XRD spectra of copper films grown on Pd films at various temperatures.

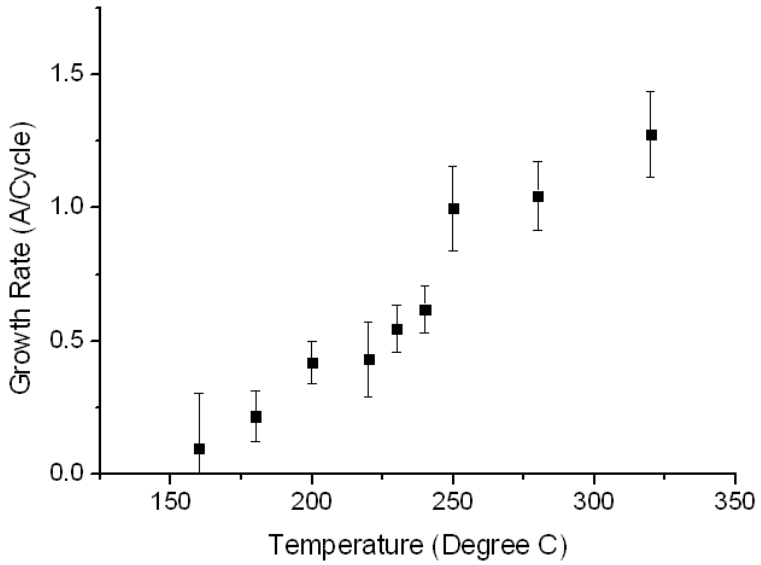

Figure 6 : Growth Rate vs temperature on Pd; the error bars refer to the standard deviation

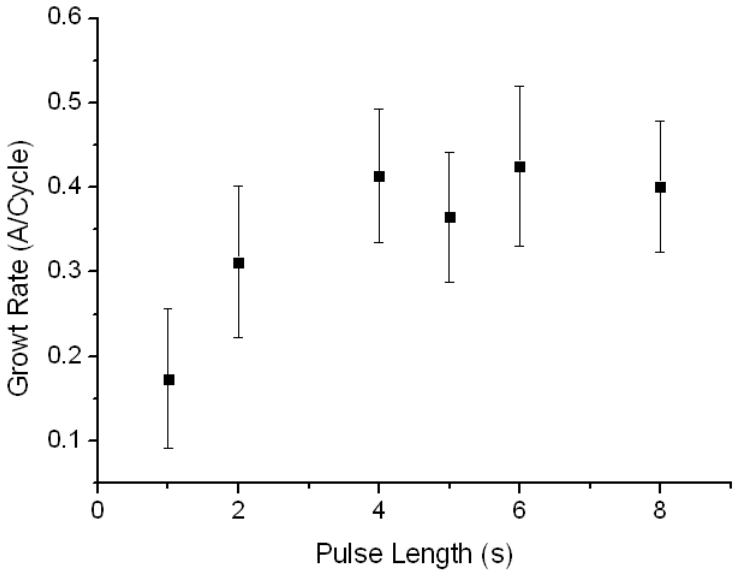

Figure 7 : Growth Rate vs precursor pulse length for Cu films grown on Pd at a substrate temperature of 220 $^{\circ}$C; the error bars refer to the standard deviation.

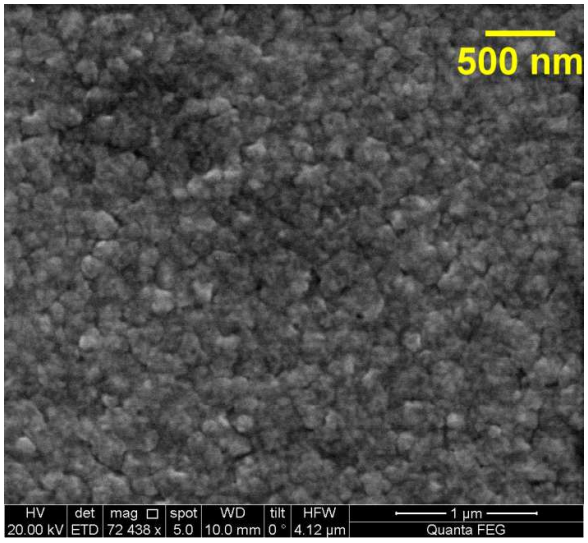

Figure 8 (a)

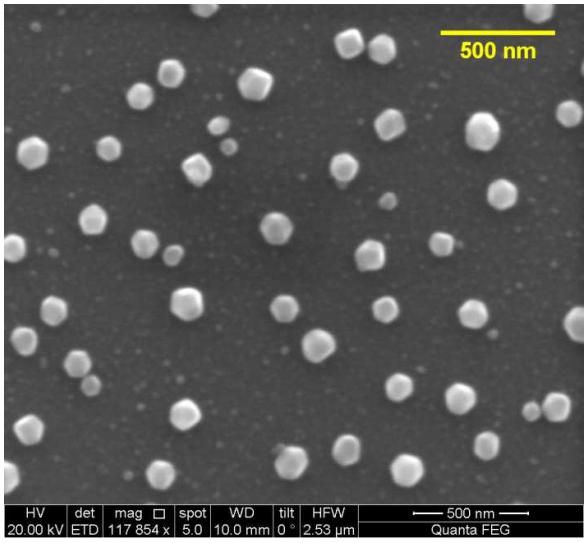

Figure 8 (b)

Figure 8 : Cu deposited on Pd films at 220 °C with 1000 cycles; the Pd films were 70 nm (a) and 10 nm (b) thick.

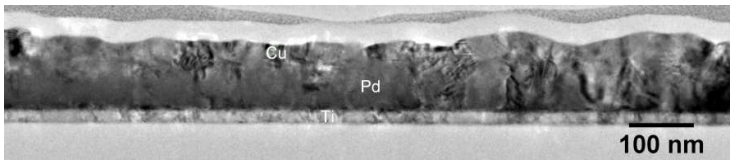

Figure 9 (a)

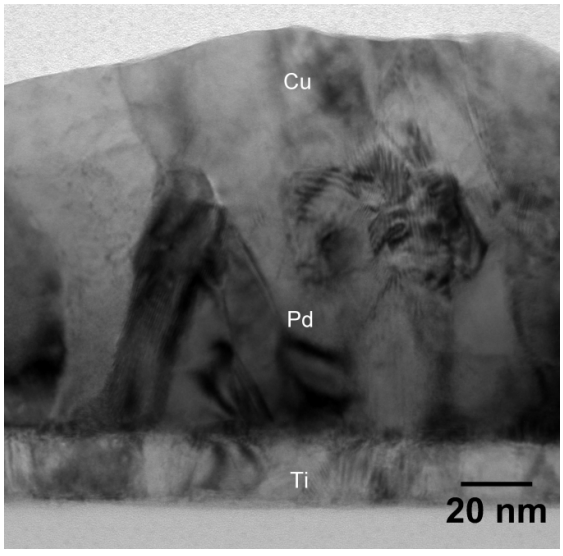

Figure 9 (b)

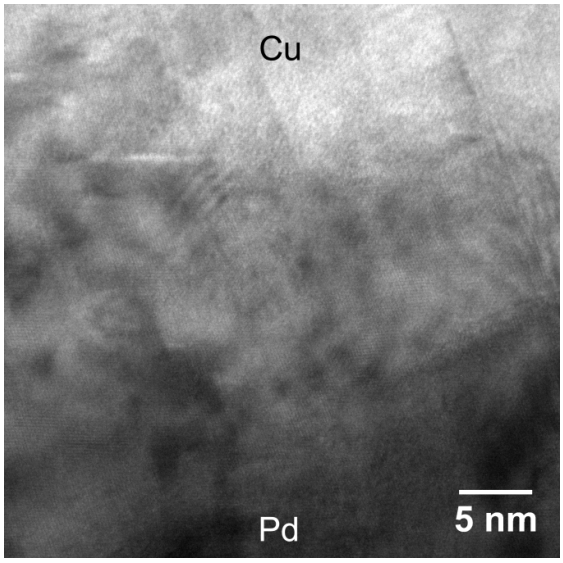

Figure 9(c)

Figure 9: TEM cross-sections of Cu films deposited on Pd at 220 °C; HR-micrograph (c) was taken from the Pd/Cu interface region.

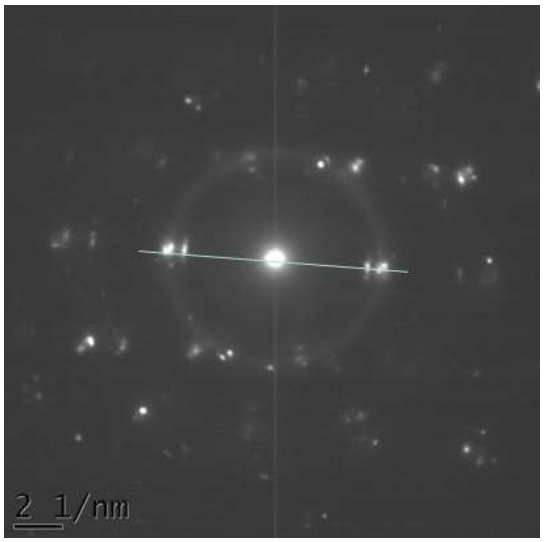

Figure 10 (a)

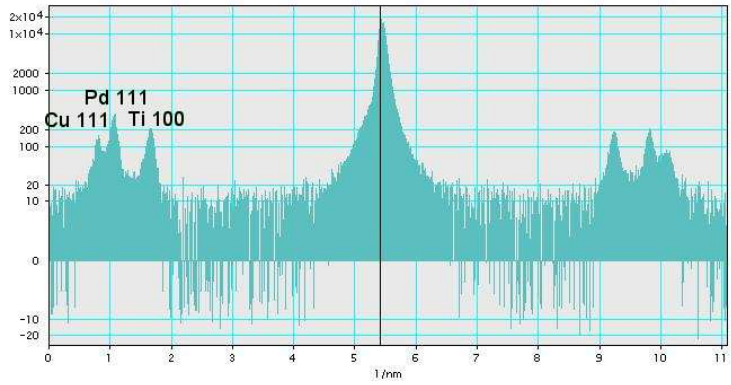

Figure 10 (b)

Figure 10: SAED pattern of Cu film deposited on Pd; (b) cross-section along blue line.

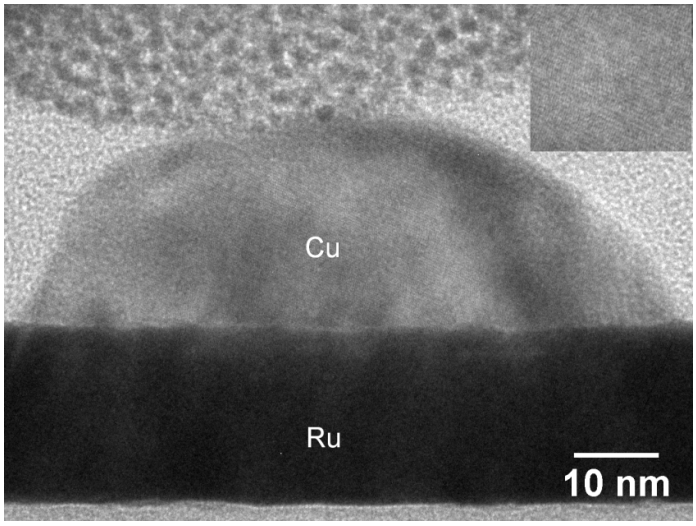

Figure 11 (a)

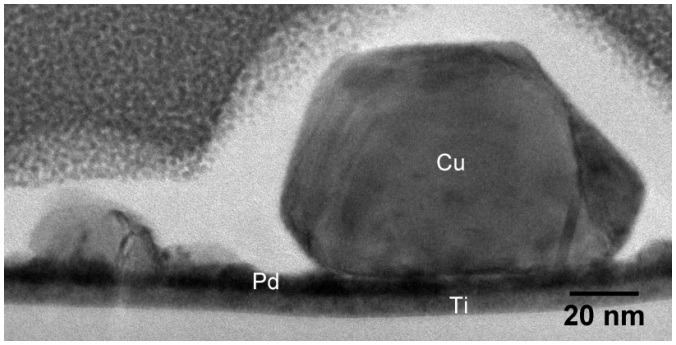

Figure 11 (b)

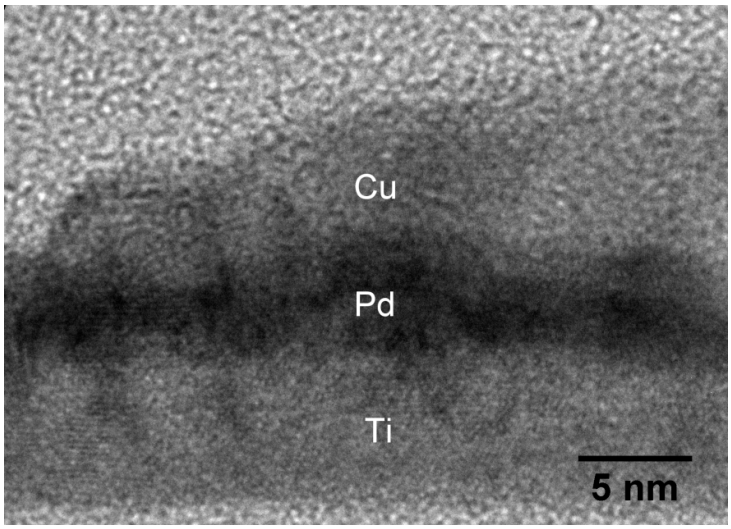

Figure 11 (c)

Figure 11: TEM cross-sections of Cu deposits grown at 220 °C on (a) Ru, and (b), (c) ultra-thin Pd: the intersect in (a) shows a magnification from the Cu island.

References

1 H. Kim and P. C. McIntyre, J. Korean Phys. Soc., 2006, 48, 5 – 17.

2 M. M. Frank, ECS Trans., 2007, 11, 187 – 200.

3 D. N. Goldstein, J. A. McCormick and S. M. George, J. Phys. Chem. C, 2008, 112, 19530 – 19539.

4 R. L. Puurunen, J. Appl. Phys., 2005, 97, 121301.

5 J. A. van Delft, D. Garcia-Alonso and W. M. M. Kessels, Semicond. Sci. Technol., 2012, 27, 074002.

6 G. Dingemans and W. M. M. Kessels, J. Vac. Sci. Technol. A, 2012, 30, 040802.

7 S. M. George, Chem. Rev., 2010, 110, 111–131.

8 R. W. Johnson, A. Hultqvist and S. F. Bent, Mater. Today, 2014, 17, 236– 246.

9 H. Kim, H.-B.-R. Lee and W.-J. Maeng, Thin Solid Films, 2009, 517, 2563–2580.

10 M. Knez, K. Nielsch and L. Niinist, Adv. Mater., 2007, 19, 3425–3438.

11 M. Leskela and M. Ritala, Thin Solid Films, 2002, 409, 138–146.

12 V. Miikkulainen, M. Leskela, M. Ritala and R. L. Puurunen, J. Appl. Phys., 2013, 113, 021301.

13 H. B. Profijt, S. E. Potts, M. C. M. van de Sanden and W. M. M. Kessels, J. Vac. Sci. Technol. A, 2011, 29, 050801.

14 K. B. Ramos, M. J. Saly and Y. J. Chabal, Coordin. Cem. Rev., 2013, in press, xxxx.

15 K. Yong and J. Jeong, Korean J. Chem. Eng., 2002, 19, 451–462.

16 F. Zaera, J. Mater. Chem., 2008, 18, 3521–3526.

17 S. M. Gates, Chem. Rev., 1996, 96, 1519–1532.

18 K. Choy, Prog. Mater. Sci., 2003, 48, 57 – 170.

19 J. R. Creighton and J. E. Parmeter, Crit. Rev. Solid State, 1993, 18, 175 –238.

20 P. O'Brien, N. L. Pickett and D. J. Ottway, Chem. Vap. Depos., 2002, 8, 237 – 249.

21 U. Helmersson, M. Lattemann, J. Bohlmark, A. P. Ehiasarian and J. T. Gudmundsson, Thin Solid Films, 2006, 513, 1–24.

22 J. T. Gudmundsson, J. Phys.: Conf. Ser., 2008, 100, 082002.

23 M. Koh, W. Mizubayashi, K. Iwamoto, H. Murakami, T. Ono, M. Tsuno, T. Mihara, K. Shibahara, S. Miyazaki and M. Hirose, IEEE T. Electron. Dev., 2001, 48, 259 – 264.

24 ITRS 2011, Front End Processes, 2011.

25 S. Klejna and S. D. Elliott, J. Nanosci. Nanotechnol., 2011, 11, 8246 – 8250.

26 S. Klejna and S. D. Elliott, J. Phys. Chem., 2012, 116, 643 – 654.

27 C. L. Hinkle, A. M. Sonnet, E. M. Vogel, S. McDonnell, G. J. Hughes, M. Milojevic, B. Lee, F. S. Aguirre-Tostado, K. J. Choi, H. C. Kim, J. Kim
and R. M. Wallace, Appl. Phys. Lett., 2008, 92, 071901.

28 M. L. Huang, Y. C. Chang, C. H. Chang, Y. J. Lee, P. Chang, J. Kwo, T. B. Wu and M. Hong, Apll. Phys. Lett., 2005, 87, 252104.

29 H. C. M. Knoops, A. J. M. Mackus, M. E. Donders, M. C. M. van de Sanden, P. H. L. Notten and W. M. M. Kessels, ECST, 2008, 16, 209–218.

30 T. Aaltonen, M. Ritala, V. Sammelselg and M. Leskelae, J. Electrochem. Soc., 2004, 151, G489 – G492.

31 J. Heo, S.-J. Won, D. Eom, S. Y. Lee, Y. B. Ahn, C. S. Hwang and H. J. Kim, Electrochem. Solid-State Lett., 2008, 11, H210–H213.

32 T. Aaltonen, M. Ritala and M. Leskela, Electrochem. Solid-State Lett., 2005, 8, C99 – C101.

33 J. Hamalainen, T. Sajavaara, E. Puukilainen, M. Ritala and M. Leskela, Chem. Mater., 2012, 24, 55 – 60.

34 C. Wilson, J. McCormick, A. Cavanagh, D. Goldstein, A. Weimer and S. George, Thin Solid Films, 2008, 516, 6175 - 6185.

35 ITRS 2011, Interconnect, 2011.

36 T. Toerndahl, M. Ottosson and J.-O. Carlsson, Thin Solid Films, 2004, 458, 129–136.

37 T. Toerndahl, J. Lub, M. Ottossona and J.-O. Carlssona, J. Cryst. Growth, 2005, 276, 102–110.

38 M. Juppo, M. Ritala and M. Leskela, J. Vac. Sci. Technol. A, 1997, 15, 2330–2333.

39 L. Wu and E. Eisenbraun, J. Electrochem. Soc., 2009, 156, H734–H739.

40 L.Wu and E. Eisenbraun, Electrochem. Solid-State Lett., 2008, 11, H107–H110.

41 M. Utriainen, M. Kroger-Laukkanen, L.-S. Johansson and L. Niinisto, Appl. Surf. Sci., 2000, 157, 151–158.

42 I. J. Hsu, B. E. McCandless, C. Weiland and B. G. Willis, J. Vac. Sci. Technol. A, 2009, 27, 660–667.

43 P. Martensson and J.-O. Carlsson, J. Electrochem. Soc., 1998, 145, 2926–2931.

44 C. Jezewski, W. A. Lanford, C. J. Wiegand, J. P. Singh, P.-I. Wang, J. J. Senkevich and T.-M. Lua, J. Electrochem. Soc., 2005, 152, C60–C64.

45 R. Solanki and B. Pathangey, Electrochem. Solid-State Lett., 2000, 3, 479–480.

46 D. Hagen, J. Connolly, R. Nagle, I. Povey, S. Rushworth, P. Carolan, P.Ma and M. Pemble, Surf. Coat. Tech., 2013, 230, 3–12.

47 C. Dussarrat, C. Lansalot-Matras, V. M. Omarjee and A. V. Korolev, US Patent No. 2012 /0321817 A1.

48 J. Mao, E. Eisenbraun, V. Omarjee, A. Korolev and C. Dussarrat, ECST, 2011, 35, 125 – 132.

49 B. H. Lee, J. K. Hwang, J. W. Nam, S. U. Lee, J. T. Kim, S.-M. Koo, A. Baunemann, R. A. Fischer and M. M. Sung, Angew. Chem. Int. Edit., 2009, 121, 4606–4609.

50 T. J. Knisley, T. C. Ariyasena, T. Sajavaara, M. J. Saly and C. H. Winter, Chem. Mater., 2011, 23, 4417 – 4419.

51 J. A. T. Norman, B. A. Muratore, P. N. Dyer, D. A. Roberts and A. K. Hochberg, VLSI Multilevel Interconnection Conference, 1991, Proceedings., Eighth International IEEE, 1991, pp. 123 – 129.

52 S. L. Cohen, M. Liehr and S. Kasi, Appl. Phys. Lett., 1992, 60, 50–52.

53 S. L. Cohen, M. Liehr and S. Kasi, Appl. Phys. Lett., 1992, 60, 1585–1587.

54 K.-K. Choi and S.-W. Rhee, J. Electrochem. Soc., 2001, 148, C473 – C478.

55 A. R. Kim, H. J. Park, K. H. Jeong, J. G. Lee, H. S. Nam, E. G. Lee and C. H. Kang, Thin Solid Films, 2009, 517, 3827 – 3830.

56 J. A. Norman, D. A. Roberts, A. K. Hochberg, P. Smith, G. A. Petersen, J. E. Parmeter, C. A. Apblett and T. R. Omstead, Thin Solid Films, 1995, 262, 46 – 51.

57 J. S. Thompson, L. Zhang, J. P. Wyre, D. J. Brill and K. G. Lloyd, Thin Solid Films, 2009, 517, 2845–2850.

58 J. S. Thompson, L. Zhang, J. P.Wyre, D. Brill and Z. Li, Organometallics, 2012, 31, 7884 – 7894.

59 C. J. Jones, d and f block chemistry, Wiley Interscience, 2002.

60 V. Krisyuk, L. Aloui, N. Prudhomme, S. Sysoev, F. Senocq, D. Samelor and C. Vahlas, Electrochem. Solid-State Lett., 2011, 14, D26 – D29.

61 J. P. Coyle, G. Dey, E. R. Sirianni, M. L. Kemell, G. P. A. Yap, M. Ritala, M. Leskela, S. D. Elliott and S. T. Barry, Chem. Mater., 2013, 25, 1232 – 1238.

62 O. Chyan, T. N. Arunagiri and T. Ponnuswamy, J. Electrochem. Soc., 2003, 150, C347–C350.

63 D. Goodman, T. E. Madey, M. Ono and J. T. Y. Jr., J. Appl. Phys., 1977, 50, 279–290.

64 P. J. F. Harris, Int. Mater. Rev., 1995, 40, 97 – 115.

65 C. G. Granqvist and R. A. Buhrman, Appl. Phys. Lett., 1975, 27, 693 – 694

66 C. Granqvist and R. Buhrman, J. Catal., 1976, 42, 477 – 479.

67 F. Fillot, Z. Tokei and G. Beyer, Surface Science, 2007, 601, 986 – 993.

68 T. P. Moffat, M. Walker, P. J. Chen, J. E. Bonevich, W. F. Egelhoff, L. Richter, C. Witt, T. Aaltonen, M. Ritala, M. Leskela and D. Josella, J. Electrochem. Soc., 2006, 153, C37–C50.

69 T. Waechtler, S. Oswald, N. Roth, A. Jakob, H. Lang, R. Ecke, S. E. Schulz, T. Gessner, A. Moskvinova, S. Schulze and M. Hietscholde, J. Electrochem. Soc., 2009, 156, H453–H459.

70 T. Waechtler, S.-F. Ding, L. Hofmann, R. Mothes, Q. Xie, S. Oswald, C. Detavernier, S. E. Schulz, X.-P. Qu, H. Lang and T. Gessner, Microelectron. Eng., 2011, 88, 684 – 689.

71 F. Senocq, A. Turgambaeva, N. Prudhomme, U. Patil, V. Krisyuk, D. Samelor, A. Gleizes and C. Vahlas, Surf. Coat. Tech., 2007, 201, 9131 – 9134.

72 A. Tungler, T. Tarnai, L. Hegediis, K. Fodor and T. Mathe, Platinum Metals Rev., 1998, 42, 108 – 115.

73 F. Harraz, S. El-Hout, H. Killa and I. Ibrahim, J. Catal., 2012, 286, 184 – 192.

74 T. Theivasanthi and M. Alagar, Archives. Phys. Res., 2010, 1, 112 – 117.

75 Z. Li, A. Rahtu and R. G. Gordon, J. Electrochem. Soc., 2006, 153, C787–C794.

76 Z. Li, R. G. Gordon, D. B. Farmer, Y. Lin and J. Vlassak, Electrochem. Solid-State Lett., 2005, 8, G182–G185.

77 A. R. Denton and N. W. Ashcroft, Phys. Rev. A, 1991, 43, 3161 – 3164.

78 M. Kiyomiya, N. Momma and I. Yasumori, Bull. Chem. Soc. Jpn., 1974, 47, 1852 – 1857.

79 J. Tabatabaei, B. Sakakini, M. Watson and K. Waugh, Catal. Lett., 1999, 59, 151 - 155.

80 H. Kim, T. Koseki, T. Ohba, T. Ohta, Y. Kojima, H. Sato and Y. Shimogaki, J. Electrochem. Soc., 2005, 152, G594 – G600.

81 A. Baskaran and P. Smereka, J. Appl. Phys., 2012, 111, 044321.

82 J. van der Merwe, Surf. Sci., 2000, 449, 151 – 166.

83 P. Zhang, Y. Sui, G. Xiao, YingnanWang, ChunzhongWang, B. Liu, G. Zoua and B. Zou, J. Mater. Chem. A, 2013, 1, 1632.

84 M. Jin, H. Zhang, Z. Xieb and Y. Xia, Energy Environ. Sci., 2012, 5, 6352.